Clim. Past Discuss., 8, 3949–3976, 2012
www.clim-past-discuss.net/8/3949/2012/
doi:10.5194/cpd-8-3949-2012

Climate of the Past Discussions

Model sensitivity to North Atlantic freshwater forcing at 8.2 ka

C. Morrill[1,2], A. N. LeGrande[3], H. Renssen[4], P. Bakker[4], and B. L. Otto-Bliesner[5]

[1]Cooperative Institute for Research in Environmental Sciences, University of Colorado, Boulder, CO, USA
[2]National Oceanic and Atmospheric Administration's National Climatic Data Center, Boulder, CO, USA
[3]NASA Goddard Institute for Space Studies and Center for Climate Systems Research, New York, NY, USA
[4]Cluster Earth & Climate, Faculty of Earth and Life Sciences, Vrije Universiteit, Amsterdam, The Netherlands
[5]Climate and Global Dynamics, National Center for Atmospheric Research, Boulder, CO, USA

Received: 31 July 2012 – Accepted: 6 August 2012 – Published: 21 August 2012

Correspondence to: C. Morrill (carrie.morrill@colorado.edu)

Published by Copernicus Publications on behalf of the European Geosciences Union.

Abstract

We compared four simulations of the 8.2 ka event to assess climate model sensitivity and skill in responding to North Atlantic freshwater perturbations. All of the simulations used the same freshwater forcing, 2.5 Sv for one year, applied to either the Hudson Bay or Labrador Sea. This freshwater pulse induced a decadal-mean slowdown of 10–25 % in the Atlantic Meridional Overturning Circulation (AMOC) of the models and caused a large-scale pattern of climate anomalies that matched proxy evidence for cooling in the Northern Hemisphere and a southward shift of the Intertropical Convergence Zone. The multi-model ensemble generated temperature anomalies that were just half as large as those from quantitative proxy reconstructions, however. Also, the duration of AMOC and climate anomalies in three of the simulations was only several decades, significantly shorter than the duration of ∼ 150 yr in the paleoclimate record. Possible reasons for these discrepancies include incorrect representation of the early Holocene climate and ocean state in the North Atlantic and uncertainties in the freshwater forcing estimates.

1 Introduction

The Atlantic Meridional Overturning Circulation (AMOC) plays a key role in the climate system, particularly through its control on heat transport and storage of carbon in the deep ocean. Changes in the AMOC can have far-reaching effects on the El Niño-Southern Oscillation (Timmermann et al., 2005), Atlantic hurricane development (Zhang and Delworth, 2006), tropical rainfall (Vellinga and Wood, 2002), and marine ecosystems (Schmittner, 2005). Model simulations of the 21st century with prescribed greenhouse gas concentrations increasing according to the Intergovernmental Panel on Climate Change (IPCC) scenario SRESA1B uniformly show a reduction in the strength of the AMOC (Schmittner et al., 2005). This multi-model ensemble yields

CPD
8, 3949–3976, 2012

a mean decrease of 25 % by 2100, but there is a large range in the individual model results that indicates substantial uncertainties in the AMOC response to climate change.

Several previous model intercomparison projects were undertaken to improve understanding of the large spread in modeled AMOC. Schmittner et al. (2005) considered the skill of nine coupled climate models in matching observations of modern hydrography. They found that the models were more successful at reproducing temperature patterns than either salinity patterns or pycnocline depth. Stouffer et al. (2006) examined the response of both Earth models of intermediate complexity (EMICs) and coupled atmosphere-ocean general circulation models (AOGCMs) to North Atlantic freshwater forcings of 0.1 and 1.0 Sv (Sverdrup = 10^6 m^3 s^{-1}) for 100 yr. While there were some robust patterns among the models, important disagreements existed in model sensitivity and in reversibility following AMOC shutdown. Since these were idealized experiments, no comparison to observations was possible. Otto-Bliesner et al. (2007) compared AMOC in four Last Glacial Maximum simulations from the second phase of the Paleoclimate Modelling Intercomparison Project (PMIP2). These models gave very different glacial circulations and a comparison to paleoclimate proxy evidence indicated serious mismatches for several of the simulations.

For the third phase of PMIP, the 8.2 ka event has been targeted for a new model intercomparison. Of past abrupt changes in the AMOC, the 8.2 ka event provides a particularly useful case study because its duration (~ 150 yr; Thomas et al., 2007) and forcing are well constrained, making an achievable target for climate model simulations (Schmidt and LeGrande, 2005). The hypothesized cause of the 8.2 ka event, haline forcing from the drainage of proglacial Lake Agassiz-Ojibway (hereafter Lake Agassiz; Barber et al., 1999) into the Hudson Bay ~ 8200 yr ago, is not a perfect analog to the thermal forcing of the AMOC predicted for the future (Gregory et al., 2005). Nonetheless, the 8.2 ka event offers a test of model sensitivity to North Atlantic surface buoyancy anomalies that has precise dating, quantified forcing, and a duration short enough to make simulations with state-of-the-art coupled climate models feasible (Schmidt and LeGrande, 2005; Thomas et al., 2007; Kobashi et al., 2007).

CPD
8, 3949–3976, 2012

Model sensitivity to North Atlantic freshwater forcing at 8.2 ka

C. Morrill et al.

2 Models and experiments

We compare 8.2 ka experiments completed with three models: the Community Climate System Model version 3 (CCSM), the Goddard Institute for Space Studies (GISS) ModelE-R and LOVECLIM version 1.2. CCSM and ModelE-R are atmosphere-ocean general circulation models (AOGCMs) coupled without flux adjustments. LOVECLIM is an Earth system model of intermediate complexity with its most significant simplifications applied to the atmosphere component (Table 1).

Of relevance to this study, the ocean models of ModelE-R and LOVECLIM are mass-conserving, in which the addition of freshwater causes a rise in the free surface of the ocean and reduces salinity purely through dilution. The ocean model component of CCSM uses the rigid-lid approximation, which does not permit vertical motion at the top of the ocean and parameterizes the addition of freshwater as a salt extraction while keeping the volume of the ocean constant. Yin et al. (2009) discuss the differences between these two approaches and compare results from two versions of the GFDL CM2.1 model using each formulation. For a large freshwater forcing that is similar in magnitude to that used in 8.2 ka experiments, the rigid-lid version exaggerates the forcing and there are significant regional biases in sea surface salinity (SSS). Despite this, the AMOC behaves similarly in the two versions and many fundamental aspects of the two simulations are qualitatively similar.

Boundary conditions specified for the control simulations are listed in Table 2. Early Holocene orbital forcing increased the seasonality of insolation in the Northern Hemisphere and decreased seasonality in the Southern Hemisphere relative to the present (Berger, 1978). Greenhouse gas concentrations for the Early Holocene were nearly identical to those for the recent pre-Industrial period (Flückiger et al., 2002; Monnin et al., 2004). Two of the control simulations, $CCSM_{all}$ and LOVECLIM, incorporated the surface albedo and elevation effects of the remnant of the Laurentide Ice Sheet that was present near Hudson Bay at 8.5 ka, as reconstructed by Peltier (2004). These same control simulations also included a small (~ 0.05 Sv) background flux of Laurentide meltwater (Licciardi et al., 1999). In $CCSM_{all}$, this freshwater flux was added to the modeled St. Lawrence River at its outflow, and was spread as a virtual salinity flux along the coast near the river's mouth. In LOVECLIM, the freshwater was added as a volume to the upper layer of the ocean at the Hudson Strait. Since the ocean model in LOVECLIM has a free surface, this effectively means that the surface height was raised. The temperature of the added freshwater in LOVECLIM was assigned the same temperature as the water in the ocean cell to which it was added. Both of these control simulations with background meltwater flux were integrated until reaching a quasi-equilibrium, in which SSS of the North Atlantic had stabilized. Global mean ocean salinity decreases slowly throughout these control simulations due to the background meltwater flux, a trend that parallels observed freshening during the late glacial and early Holocene. A second CCSM control simulation ($CCSM_{og}$; OG = orbital and greenhouse gas only) without a Laurentide Ice Sheet and background meltwater flux is included in this study for a more direct comparison to ModelE-R results.

For the 8.2 ka event experiments, a meltwater pulse (MWP) of 2.5 Sv for 1 yr was added to each of the control simulations to represent the drainage of Lake Agassiz. This freshwater volume was the best estimate for the drainage event based on flood hydrograph simulations (Clarke et al., 2004). Following the one-year perturbation, the MWP ceased and the climate was allowed to recover. In the models with a free-surface ocean, the MWP was added as a volume to a limited number of grid cells. In ModelE-R, freshwater was added to the approximately 20 grid boxes in the Hudson Bay and was assigned a temperature of 0 °C. In LOVECLIM, freshwater was added to the upper layers of the ocean at the Hudson Strait and was assigned the same temperature as the water in the ocean cell to which it was added. The virtual salinity flux in CCSM required a larger area for the MWP (50–65° N, 35–70° W).

The control simulation for ModelE-R displayed a number of transient, quasi-stable states with either strong or weak AMOC (LeGrande et al., 2006; LeGrande and Schmidt, 2008). For this study, we use an experiment begun from a period of weak AMOC. Since the weak case exhibits some high amplitude decadal variability, we reduced the influence of this unforced variability through examining "decadal" results for this model (i.e., the 10-yr mean of the MWP experiment less the 30-yr mean of the relevant control years).

3 Response to freshwater forcing

3.1 AMOC

AMOC intensity is defined here as the maximum of the Atlantic overturning streamfunction excluding the surface (< 500 m) wind-driven overturning circulation. Mean values for the control simulations range from 16 to 20 Sv (Fig. 1), and interannual variability is small in the three simulations with available annual output (standard deviations: LOVECLIM = 0.7, $CCSM_{og}$ = 1.1, $CCSM_{all}$ = 0.9 Sv). AMOC intensity is lower by several Sv in the simulations with a background meltwater flux. AMOC has a similar structure in all the control simulations. The northward flow of warm, salty water occurs in the upper 1000 m, while the southward return flow of North Atlantic Deep Water occurs between 1000–3000 m. The anticlockwise cell in the deep ocean, associated with Antarctic Bottom Water formation, has a strength of about 4 Sv in all control simulations.

The values of AMOC intensity in the control simulations are generally similar to the strength of the modern-day AMOC (Meehl et al., 2007). Proxy evidence suggests that the strength of the AMOC during the early Holocene was probably not that different from today (Bianchi and McCave, 1999; Hall et al., 2004; Oppo et al., 2003; McManus et al., 2004; Praetorius et al., 2008). There is some proxy evidence for lack of convection and deep water formation in the Labrador Sea during the early Holocene, however (e.g., Hillaire-Marcel et al., 2001; Solignac et al., 2004; Fagel et al., 2004). Of the four experiments we compare, only the CCSM experiments have some convection in the general region of the Labrador Sea (not shown).

Following the 2.5 Sv MWP for one year, AMOC intensity decreases in all simulations (Fig. 2). The maximum decadal-mean decline in LOVECLIM and CCSM is about 10 %,

CPD
8, 3949–3976, 2012

while for ModelE-R it is about 25 %. The decline in AMOC intensity in LOVECLIM and CCSM is relatively short-lived, on the order of several decades, and generally within the range of natural variability of AMOC in their control simulations. The response in ModelE-R is more pronounced and longer-lived, extending on the order of 100–120 yr. Proxy records do not provide a quantitative estimate of AMOC weakening at 8.2 ka, but do suggest a duration of 100–200 yr (Ellison et al., 2006; Kleiven et al., 2008).

3.2 Ocean salinity and temperature

Significant freshening of the North Atlantic occurs following the MWP in all simulations (Fig. 3). The largest anomalies are generally along the coast of Labrador and are up to 1 psu when averaged over the first fifty years following the MWP. From the Labrador Sea, freshwater travels eastward into the North Atlantic in all simulations. For most of the simulations, it appears that then a significant amount enters the Greenland-Iceland-Norwegian Seas and a somewhat smaller amount is entrained in the subtropical gyre. This pathway is different from that inferred by Keigwin et al. (2005), who used δ^{18}O of planktic foraminifera to suggest salinity was decreased near Cape Hatteras around 8.2 ka. Also, it has been argued that freshwater released from Hudson Strait would be trapped along the North American coast and would not easily escape to the open North Atlantic (e.g., Wunsch, 2010). However, there is evidence from several proxy records that combine δ^{18}O and Mg/Ca of planktic foraminera to infer freshening in the Irminger and Labrador Seas of up to 1 psu at 8.2 ka (Came et al., 2007; Hoffmann et al., 2012; Winsor et al., 2012; Thornalley et al., 2009). Areas of positive SSS anomalies at the mouth of the St. Lawrence River in CCSM$_{all}$ are caused by cessation of the 0.05 Sv background meltwater flux once Lake Agassiz has drained. Globally, negative anomalies greater than 0.2 psu are confined to the North Atlantic and Arctic oceans (not shown).

Likewise, sea surface cooling is concentrated in the North Atlantic in all simulations (Fig. 4). Mean anomalies across the North Atlantic for the first fifty years following the MWP are on the order of 1 °C, though they exceed 2 °C locally in the CCSM and

CPD
8, 3949–3976, 2012

ModelE-R experiments. Maximum anomalies in the LOVECLIM simulation are on the order of ∼0.5 °C and are located in the far North Atlantic. ModelE-R shows cooling on the order of several tenths of a degree Celsius across most of the Southern Hemisphere. The other simulations show little significant change south of 30° N with the exception of $CCSM_{all}$, which has some significant warming in the south Atlantic.

3.3 Sea ice

All of the simulations have areas of significantly expanded sea ice following freshwater forcing, particularly in the Labrador Sea and in the Norwegian and/or Barents Sea (Fig. 5). Generally, these changes for the first fifty years following the MWP are on the order of 5–10 %, although they can be as large as 20–25 % in some areas. Sea ice changes in the Southern Ocean have a heterogeneous spatial pattern and generally are not statistically significant.

3.4 Surface air temperature

The North Atlantic region and the Arctic become significantly colder in most simulations during the first fifty years following the MWP, with mean annual temperatures in the multi-model ensemble decreasing less than ∼0.5 °C over Europe and ∼1.0 °C over Greenland (Fig. 6). These results hold for individual ensemble members, as well, for both Europe (40–60° N, 10° W–30° E; anomalies are LOVECLIM = 0.0 °C, CCSMog = −0.3 °C, CCSMall = −0.5 °C, ModelE-R = −0.6 °C) and Greenland (60–80° N, 60–20° W; anomalies are LOVECLIM = 0.0 °C, CCSMog = −0.6 °C, CCSMall = −0.4 °C, ModelE-R = −0.8 °C). Temperature changes are minimal in the tropics and the Southern Hemisphere. This spatial pattern agrees well with proxy records, which clearly indicate colder conditions across the Northern Hemisphere during the 8.2 ka event but suggest that any Southern Hemisphere temperature changes were likely regional (Fig. 6).

CPD
8, 3949–3976, 2012

Title Page
Abstract | Introduction
Conclusions | References
Tables | Figures
◂| |▸
◂ ▸
Back | Close
Full Screen / Esc
Printer-friendly Version
Interactive Discussion

The magnitude of circum-North Atlantic temperature changes inferred from proxies is somewhat larger than those in the models. Temperature reconstructions from pollen and δ^{18}O in Europe consistently show anomalies of about −1.1 to −1.2 °C in mean annual temperature during the 8.2 ka event (Veski et al., 2004; von Grafenstein et al., 1998; Sarmaja-Korjonen and Seppä, 2007; Feurdean et al., 2008). Nitrogen isotopes from Greenland indicate temperatures decreased about 2.2 °C averaged over the duration of the event, with an even larger decrease of 3.3 °C during the most extreme 60-yr period (Kobashi et al., 2007).

Anomalies over the North Atlantic in the LOVECLIM and CCSM experiments are short-lived; generally, temperature values are outside the range of natural variability (defined as the mean ± 2 standard deviations of the control) for less than two decades (Fig. 7). Anomalies are longer-lived in the ModelE-R simulation, lasting on the order of 100 yr. These longer-lived anomalies are a better match to high-resolution proxy records from Europe and Greenland, which consistently show an event duration of 100 to 150 yr (Morrill et al., 2012).

3.5 Precipitation

Despite the noise inherent in precipitation, a number of features are common among the model simulations for the fifty years following the MWP. In all cases, the most important changes are a reduction in precipitation over the North Atlantic and Northern Hemisphere tropics, and an increase in precipitation over the Southern Hemisphere tropics (Fig. 8). The tropical pattern, consistent with a southward shift of the mean position of the Intertropical Convergence Zone, is clearest over the Atlantic Ocean (Fig. 9). Tropical proxy records from both speleothem δ^{18}O measurements and indicators of lake water balance support this spatial pattern (Fig. 8).

Several quantitative estimates of drying exist from proxies in high northern latitudes; these include an ~ 8 % reduction in accumulation in central Greenland ice cores and an ~ 17 % reduction in rainfall inferred from pollen north of the Mediterranean (Feurdean et al., 2008; Pross et al., 2009; Hammer et al., 1997; Rasmussen et al., 2007). The model

CPD
8, 3949–3976, 2012

simulations generally match the magnitude of drying in central Greenland, but typically do not match either the direction or magnitude of change in southeastern Europe. Additionally, evidence for wetter conditions at 8.2 ka from pollen and lake geochemical records in northern Europe is not matched by the freshwater experiments (Fig. 8).

4 Discussion and conclusions

To summarize, the models generally do a good job in reproducing large-scale patterns of temperature and precipitation changes at 8.2 ka inferred from proxy records. These patterns include cooling across most of the Northern Hemisphere and a southward shift of the Intertropical Convergence Zone. The models have less success in matching the magnitude and duration of climate anomalies. Temperature changes in the multi-model ensemble are about half the size of those of quantitative proxy records from Europe and Greenland. For all but one of the simulations, the duration of the 8.2 ka climate anomalies is on the order of several decades rather than the ~ 150 yr observed in proxy records. Also, there are discrepancies between model and data for some regional-scale anomaly patterns, including precipitation changes in Europe. These patterns are less well-constrained by proxy evidence, however.

The background climate state of the early Holocene, and the location of convection areas in the North Atlantic more specifically, might explain some of the differences we see between models and proxy data. The ModelE-R simulation has the best match to proxies for event duration, and it has been previously demonstrated for this model that the lack of Labrador Sea convection is essential for this response (LeGrande and Schmidt, 2008; LeGrande et al., 2006). Previous work with the ECBilt-CLIO model also supports this interpretation; when Labrador Sea convection is weak in that model, the ocean's ability to transport freshwater anomalies away from the North Atlantic is diminished and the response to freshwater forcing is prolonged (Wiersma et al., 2006). On the other hand, lack of convection in the Labrador Sea does not lead to a long-lived climate response in the LOVECLIM experiment. Plus, proxies indicate that AMOC

CPD
8, 3949–3976, 2012

strength was not too different from today during the early Holocene. In this case, some other convection area, perhaps in the Irminger Basin, might have been stronger in the early Holocene to offset the weaker Labrador Sea convection (Hall et al., 2010). If this was true, the strengthened convection areas elsewhere might be able to compensate for decreased freshwater divergence in the Labrador Sea.

Another factor in the model-data mismatch could be the size of the MWP. The model simulations were forced with 2.5 Sv for one year, which was the best estimate of the flood hydrograph simulations of Clarke et al. (2004). As these authors point out, though, the total volume of Lake Agassiz would have generated twice this forcing (Teller et al., 2002). Their flood model generates a stable drainage channel that prohibits complete drainage, but this result might be unlikely for an outburst flood from Lake Agassiz. Reconstructions of sea level rise at 8.2 ka support the idea of a larger freshwater drainage. Using peat deposits from the Mississippi River delta, Li et al. (2012) reconstructed a total eustatic sea level rise of 0.8 to 2.2 m at 8.2 ka. This is significantly larger than the forcing of 2.5 Sv for one year (~ 0.2 m sea level equivalent) or even than the entire volume of Lake Agassiz (~ 0.4 m sea level equivalent).

The difference in boundary conditions between the control simulations does not obviously account for divergent model responses. As shown in the comparison of the two CCSM simulations, $\mathrm{CCSM_{og}}$ and $\mathrm{CCSM_{all}}$, the addition of a remnant Laurentide Ice Sheet and a background meltwater flux does not alter the model response to freshwater forcing, either in magnitude or duration. It is worth noting, however, that these boundary conditions were important in previous experiments with ECBilt-Clio for prolonging the AMOC response to Lake Agassiz drainage (Wiersma et al., 2006). Thus, the effects of these boundary conditions might be very model-dependent. Differences between early Holocene and preindustrial orbital forcing and greenhouse gas concentrations are relatively minor, and are not expected to have an important influence. This should be verified, though, with additional model experiments.

A last explanation for the model-data discrepancies is that the models are not sensitive enough to freshwater perturbations. If true, this finding would have important

CPD
8, 3949–3976, 2012

implications for future climate projections, particularly as models suggest that continued melting of the Greenland Ice Sheet at its current rate will have a significant impact on the AMOC (Hu et al., 2009). Improved constraints on the size of freshwater forcing and its location with respect to early Holocene convection areas are necessary to rule out the possibility of inadequate model sensitivity.

Acknowledgements. Funding for the CCSM simulations was provided by a grant from the US National Science Foundation, Office of Polar Programs, to CM and BLOB and supercomputer time was provided by a grant from the National Center for Atmospheric Research (NCAR) Computational Information Systems Laboratory (CISL). We thank Nan Rosenbloom for running the $CCSM_{all}$ simulations, Ellen Ward for assistance with figures, and Amy Wagner for helpful discussions.

References

Barber, D. C., Dyke, A., Hillaire-Marcel, C., Jennings, A. E., Andrews, J. T., Kerwin, M. W., Bilodeau, G., McNeely, R., Southon, J., Morehead, M. D., and Gagnon, J.-M.: Forcing of the cold event of 8,200 years ago by catastrophic drainage of Laurentide lakes, Nature, 400, 344–348, 1999.

Berger, A. L.: Long-term variations of caloric insolation resulting from the Earth's orbital elements, Quatern. Res., 9, 139–167, 1978.

Bianchi, G. G. and McCave, I. N.: Holocene periodicity in North Atlantic climate and deep-ocean flow south of Iceland, Nature, 397, 515–517, 1999.

Came, R. E., Oppo, D. W., and McManus, J. F.: Amplitude and timing of temperature and salinity variability in the subpolar North Atlantic over the past 10 k.y., Geology, 35, 315–318, 2007.

Clarke, G. K. C., Leverington, D. W., Teller, J. T., and Dyke, A. S.: Paleohydraulics of the last outburst flood from glacial Lake Agassiz and the 8200 BP cold event, Quaternary Sci. Rev., 23, 389–407, 2004.

Collins, W. D., Bitz, C. M., Blackmon, M. L., Bonan, G. B., Bretherton, C. S., Carton, J. A., Chang, P., Doney, S. C., Hack, J. J., Henderson, T. B., Kiehl, J. T., Large, W. G., McKenna, D. S., Santer, B. D., and Smith, R. D.: The Community Climate System Model Version 3 (CCSM3), J. Climate, 19, 2122–2143, 2006.

Ellison, C. R. W., Chapman, M. R., and Hall, I. R.: Surface and deep ocean interactions during the cold climate event 8200 years ago, Science, 312, 1929–1932, 2006.
Fagel, N., Hillaire-Marcel, C., Humblet, M., Brasseur, R., Weis, D., and Stevenson, R.: Nd and Pb isotope signatures of the clay-size fraction of Labrador Sea sediments during the Holocene: Implications for the inception of the modern deep circulation pattern, Paleoceanography, 19, PA3002, doi:10.1029/2003PA000993, 2004.
Feurdean, A., Klotz, S., Mosbrugger, V., and Wolhfarth, B.: Pollen-based quantitative reconstructions of Holocene climate variability in NW Romania, Palaeogeogr. Palaeoclim., 260, 494–504, 2008.
Flückiger, J., Monnin, E., Stauffer, B., Schwander, J., Stocker, T. F., Chappellaz, J., Raynaud, D., and Barnola, J.-M.: High-resolution Holocene N_2O ice core record and its relationship with CH_4 and CO_2, Global Biogeochem. Cy., 16, 1010, doi:10.1029/2001GB001417, 2002.
Goosse, H., Brovkin, V., Fichefet, T., Haarsma, R., Huybrechts, P., Jongma, J., Mouchet, A., Selten, F., Barriat, P.-Y., Campin, J.-M., Deleersnijder, E., Driesschaert, E., Goelzer, H., Janssens, I., Loutre, M.-F., Morales Maqueda, M. A., Opsteegh, T., Mathieu, P.-P., Munhoven, G., Pettersson, E. J., Renssen, H., Roche, D. M., Schaeffer, M., Tartinville, B., Timmermann, A., and Weber, S. L.: Description of the Earth system model of intermediate complexity LOVECLIM version 1.2, Geosci. Model Dev., 3, 603–633, doi:10.5194/gmd-3-603-2010, 2010.
Gregory, J. M., Dixon, K. W., Stouffer, R. J., Weaver, A. J., Driesschaert, E., Eby, M., Fichefet, T., Hasumi, H., Hu, A., Jungclaus, J. H., Kamenkovich, I. V., Levermann, A., Montoya, M., Murakami, S., Nawrath, S., Oka, A., Sokolov, A. P., and Thorpe, R. B.: A model intercomparison of changes in the Atlantic thermohaline circulation in response to increasing atmospheric CO2 concentration, Geophys. Res. Lett., 32, L12703, doi:10.1029/2005GL023209, 2005.
Hall, I. R., Bianchi, G. G., and Evans, J. R.: Centennial to millennial scale Holocene climate-deep water linkage in the North Atlantic, Quaternary Sci. Rev., 23, 1529–1536, 2004.
Hall, I. R., Becker, J., Thornalley, D., and Hemming, S. R.: Holocene variability of North Atlantic deep water: palaeocurrent reconstruction of component water masses close to their source, 10th International Conference on Paleoceanography, La Jolla, CA, 2010.
Hammer, C. U., Andersen, K. K., Clausen, H. B., Dahl-Jensen, D., Hvidberg, C. S., and Iversen, P.: The stratigraphic dating of the GRIP ice core, Special Report of the Geophysical Department, Niels Bohr Institute for Astronomy, Physics and Geophysics, University of Copenhagen, 1997.

CPD
8, 3949–3976, 2012

Model sensitivity to North Atlantic freshwater forcing at 8.2 ka

C. Morrill et al.

Hillaire-Marcel, C., de Vernal, A., Bilodeau, G., and Weaver, A. J.: Absence of deep-water formation in the Labrador Sea during the last interglacial period, Nature, 410, 1073–1077, 2001.
Keigwin, L. D., Sachs, J. P., Rosenthal, Y., and Boyle, E. A.: The 8200 yr BP event in the slope water system, western subpolar North Atlantic, Paleoceanography, 20, PA001074, doi:10.1029/2004PA001074, 2005.
Kleiven, H. F., Kissel, C., Laj, C., Ninnemann, U. S., Richter, T. O., and Cortijo, E.: Reduced North Atlantic Deep Water coeval with the Glacial lake Agassiz freshwater outburst, Science, 319, 60–64, 2008.
Kobashi, T., Severinghaus, J. P., Brook, E. J., Barnola, J.-M., and Grachev, A. M.: Precise timing and characterization of abrupt climate change 8200 years ago from air trapped in polar ice, Quaternary Sci. Rev., 26, 1212–1222, 2007.
LeGrande, A. N. and Schmidt, G. A.: Ensemble, water isotope-enabled, coupled general circulation modeling insights into the 8.2 ka event, Paleoceanography, 23, PA3207, doi:10.1029/2008PA001610, 2008.
LeGrande, A. N., Schmidt, G. A., Shindell, D. T., Field, C. V., Miller, R. L., Koch, D. M., Faluvegi, G., and Hoffmann, G.: Consistent simulations of multiple proxy responses to an abrupt climate change event, P. Natl. Acad. Sci., 103, 837–842, 2006.
Li, Y.-X., Tornqvist, T. E., Nevitt, J. M., and Kohl, B.: Synchronizing a sea-level jump, final Lake Agassiz drainage, and abrupt cooling 8200 years ago, Earth Planet. Sc. Lett., 315–316, 41–50, 2012.
Licciardi, J. M., Teller, J. T., and Clark, P. U.: Freshwater routing by the Laurentide ice sheet during the last deglaciation, in: Mechanisms of Global Climate Change at Millennial Time Scales, edited by: Clark, P. U., Webb, R. S., and Keigwin, L. D., American Geophysical Union, Washington, D.C., 177–201, 1999.
McManus, J. F., Francois, R., Gherardi, J.-M., Keigwin, L. D., and Brown-Leger, S.: Collapse and rapid resumption of Atlantic meridional circulation linked to deglacial climate changes, Nature, 428, 834–837, 2004.
Meehl, G. A., Stocker, T. F., Collins, W. D., Friedlingstein, P., Gaye, A. T., Gregory, J. M., Kitoh, A., Knutti, R., Murphy, J. M., Noda, A., Raper, S. C. B., Watterson, I. G., Weaver, A. J., and Zhao, Z.-C.: Global Climate Projections, in: Climate Change 2007: The Physical Science Basis, Contribution of Working Group I to the Fourth Assessment Report of the Intergovernmental Panel on Climate Change, edited by: Solomon, S., Qin, D., Manning, M., Chen, Z.,

Marquis, M., Averyt, K. B., Tignor, M., and Miller, H. L., Cambridge University Press, New York, N.Y., 747–846, 2007.

Monnin, E., Steig, E. J., Siegenthaler, U., Kawamura, K., Schwander, J., Stauffer, B., Stocker, T. F., Morse, D. L., Barnola, J.-M., Bellier, B., Raynaud, D., and Fischer, H.: Evidence for substantial accumulation rate variability in Antarctica during the Holocene, through synchronization of CO_2 in the Taylor Dome, Dome C and DML ice cores, Earth Planet. Sc. Lett., 224, 45–54, 2004.

Oppo, D. W., McManus, J. F., and Cullen, J. L.: Deepwater variability in the Holocene epoch, Nature, 422, 277–278, 2003.

Otto-Bliesner, B. L., Brady, E. C., Clauzet, G., Tomas, R., Levis, S., and Kothavala, Z.: Last Glacial Maximum and Holocene climate in CCSM3, J. Climate, 19, 2526–2544, 2006.

Otto-Bliesner, B. L., Hewitt, C. D., Marchitto, T. M., Brady, E., Abe-Ouchi, A., Crucifix, M., Murakami, S., and Weber, S. L.: Last Glacial Maximum ocean thermohaline circulation: PMIP2 model intercomparisons and data constraints, Geophys. Res. Lett., 34, L12706, doi:10.1029/2007GL029475, 2007.

Peltier, W. R.: Global glacial isostasy and the surface of the ice-age Earth: the ICE-5G (VM2) model and GRACE, Annu. Rev. Earth Planet. Sci., 32, 111–149, 2004.

Praetorius, S., McManus, J. F., Oppo, D. W., and Curry, W. B.: Episodic reductions in bottom-water currents since the last ice age, Nat. Geosci., 1, 449–452, 2008.

Pross, J., Kutthoff, U., Muller, U. C., Peyron, O., Dormoy, I., Schmiedl, G., Kalaitzidis, S., and Smith, A. M.: Massive perturbation in terrestrial ecosystems of the Eastern Mediterranean region associated with the 8.2 kyr B.P. climatic event, Geology, 37, 887–890, 2009.

Rasmussen, S. O., Vinther, B. M., Clausen, H. B., and Andersen, K. K.: Early Holocene climate oscillations recorded in three Greenland ice cores, Quaternary Sci. Rev., 26, 1907–1914, 2007.

Russell, G. L., Miller, J. R., and Rind, D.: A coupled atmosphere-ocean model for transient climate change studies, Atmos.-Ocean, 33, 683–730, 1995.

Russell, G. L., Miller, J. R., Rind, D., Ruedy, R. A., Schmidt, G. A., and Sheth, S.: Comparison of model and observed regional temperature changes during the past 40 years, J. Geophys. Res., 105, 14891–14898, doi:10.1029/2000JD900156, 2000.

Sarmaja-Korjonen, K. and Seppä, H.: Abrupt and consistent responses of aquatic and terrestrial ecosystems to the 8200 cal. yr cold event: a lacustrine record from Lake Arapisto, Finland, Holocene, 17, 457–467, 2007.

CPD
8, 3949–3976, 2012

Model sensitivity to North Atlantic freshwater forcing at 8.2 ka

C. Morrill et al.

Schmidt, G. A. and LeGrande, A. N.: The Goldilocks abrupt climate change event, Quaternary Sci. Rev., 24, 1109–1110, 2005.
Schmidt, G. A., Ruedy, R., Hansen, J. E., Aleinov, I., Bell, N., Bauer, M., Bauer, S., Cairns, B., Canuto, V., Cheng, Y., Del Genio, A., Faluvegi, G., Friend, A. D., Hall, T. M., Hu, Y., Kelley, M., Kiang, N. Y., Koch, D., Lacis, A. A., Lerner, J., Lo, K. K., Miller, R. L., Nazarenko, L., Oinas, V., Perlwitz, J. P., Perlwitz, J., Rind, D., Romanou, A., Russell, G. L., Sato, M., Shindell, D. T., Stone, P. H., Sun, S., Tausnev, N., Thresher, D., and Yao, M.-S.: Present day atmospheric simulations using GISS ModelE: Comparison to in-situ, satellite and reanalysis data, J. Climate, 19, 153–192, doi:10.1175/JCLI3612.1, 2006.
Schmittner, A.: Decline of the marine ecosystem caused by a reduction in the Atlantic overturning circulation, Nature, 434, 628–633, 2005.
Schmittner, A., Latif, M., and Schneider, B.: Model projections of the North Atlantic thermohaline circulation for the 21st century assessed by observations, Geophys. Res. Lett., 32, L23710, doi:10.1029/2005GL024368, 2005.
Solignac, S., deVernal, A., and Hillaire-Marcel, C.: Holocene sea-surface conditions in the North Atlantic – contrasted trends and regimes in the western and eastern sectors (Labrador Sea vs. Iceland Basin), Quaternary Sci. Rev., 23, 319–334, 2004.
Stouffer, R. J., Yin, J., Gregory, J. M., Dixon, K. W., Spelman, M. J., Hurlin, W., Weaver, A. J., Eby, M., Flato, G. M., Hasumi, H., Hu, A., Jungclaus, J. H., Kamenkovich, I. V., Levermann, A., Montoya, M., Murakami, S., Nawrath, S., Oka, A., Peltier, W. R., Robitaille, D. Y., Sokolov, A., Vettoretti, G., and Weber, S. L.: Investigating the causes of the response of the thermohaline circulation to past and future climate changes, J. Climate, 19, 1365–1387, 2006.
Teller, J. T., Leverington, D. W., and Mann, J. D.: Freshwater outbursts to the oceans from glacial Lake Agassiz and their role in climate change during the last deglaciation, Quaternary Sci. Rev., 21, 879–887, 2002.
Thomas, E. R., Wolff, E. W., Mulvaney, R., Steffensen, J. P., Johnsen, S. J., Arrowsmith, C., White, J. W. C., Vaughn, B., and Popp, T.: The 8.2 ka event from Greenland ice cores, Quaternary Sci. Rev., 26, 70–81, 2007.
Thornalley, D. J. R., Elderfield, H., and McCave, I. N.: Holocene oscillations in temperature and salinity of the surface subpolar North Atlantic, Nature, 457, 711–714, 2009.
Timmermann, A., An, S.-I., Krebs, U., and Goosse, H.: ENSO suppression due to weakening of the North Atlantic thermohaline circulation, J. Climate, 18, 3122–3139, 2005.

CPD
8, 3949–3976, 2012

Model sensitivity to North Atlantic freshwater forcing at 8.2 ka

C. Morrill et al.

Vellinga, M. and Wood, R. A.: Global climatic impacts of a collapse of the Atlantic thermohaline circulation, Climatic Change, 54, 251–267, 2002.
Veski, S., Seppä, H., and Ojala, A. E. K.: Cold event at 8200 yr BP recorded in annually laminated lake sediments in eastern Europe, Geology, 32, 681–684, 2004.
von Grafenstein, U., Erlenkeuser, H., Muller, J., Jouzel, J., and Johnsen, S.: The cold event 8200 years ago documented in oxygen isotope records of precipitation in Europe and Greenland, Clim. Dynam., 14, 73–81, 1998.
Wiersma, A. P., Renssen, H., Goosse, H., and Fichefet, T.: Evaluation of different freshwater forcing scenarios for the 8.2 ka BP event in a coupled climate model, Clim. Dynam., 27, 831–849, 2006.
Wunsch, C.: Towards understanding the Paleocean, Quaternary Sci. Rev., 29, 1960–1967, 2010.
Yin, J., Stouffer, R. J., Spelman, M. J., and Griffies, S. M.: Evaluating the uncertainty induced by the virtual salt flux assumption in climate simulations and future projections, J. Climate, 23, 80–96, 2009.
Zhang, R. and Delworth, T. L.: Impact of Atlantic multidecadal oscillations on India/Sahel rainfall and Atlantic hurricanes, Geophys. Res. Lett., 33, L17712, doi:10.1029/2006GL026267, 2006.

Table 1. Participating models.

Model	Atmospheric model	Oceanic model	Citations
CCSM3	CAM3: T42 ($\sim 2.8^\circ \times 2.8^\circ$), 26 levels	POP: $\sim 1^\circ \times \sim 1^\circ$; $\sim 0.3^\circ \times \sim 0.3^\circ$ in North Atlantic, 40 levels, volume-conserving	Collins et al. (2006) Otto-Bliesner et al. (2006) Wagner et al. (2012)
GISS ModelE-R	ModelE: M20 ($4^\circ \times 5^\circ$), 20 levels	Russell: $4^\circ \times 5^\circ$, 13 levels, mass-conserving	Schmidt et al. (2006) Russell et al. (1995, 2000) LeGrande et al. (2006) LeGrande and Schmidt (2008)
LOVECLIM1.2	ECBilt2: T21 ($5.625^\circ \times 5.625^\circ$), 3 levels	CLIO3: $3^\circ \times 3^\circ$, 20 levels, mass-conserving	Goosse et al. (2010)

Table 2. Boundary conditions for control simulations.

Simulation	Orbital parameters	Greenhouse gas concentrations	Ice sheet	Background meltwater flux
$CCSM_{og}$	8.5 ka	$CO_2 = 260$ ppm $CH_4 = 660$ ppb $N_2O = 260$ ppb	none	none
$CCSM_{all}$	8.5 ka	$CO_2 = 260$ ppm $CH_4 = 660$ ppb $N_2O = 260$ ppb	ICE-5G	0.05 Sv added to St. Lawrence River
ModelE-R	1880 AD	$CO_2 = 285$ ppm $CH_4 = 791$ ppb $N_2O = 275$ ppb	none	none
LOVECLIM	1880 AD	$CO_2 = 280$ ppm $CH_4 = 760$ ppb $N_2O = 270$ ppb	ICE-5G	0.05 Sv added to Hudson Strait

CPD
8, 3949–3976, 2012

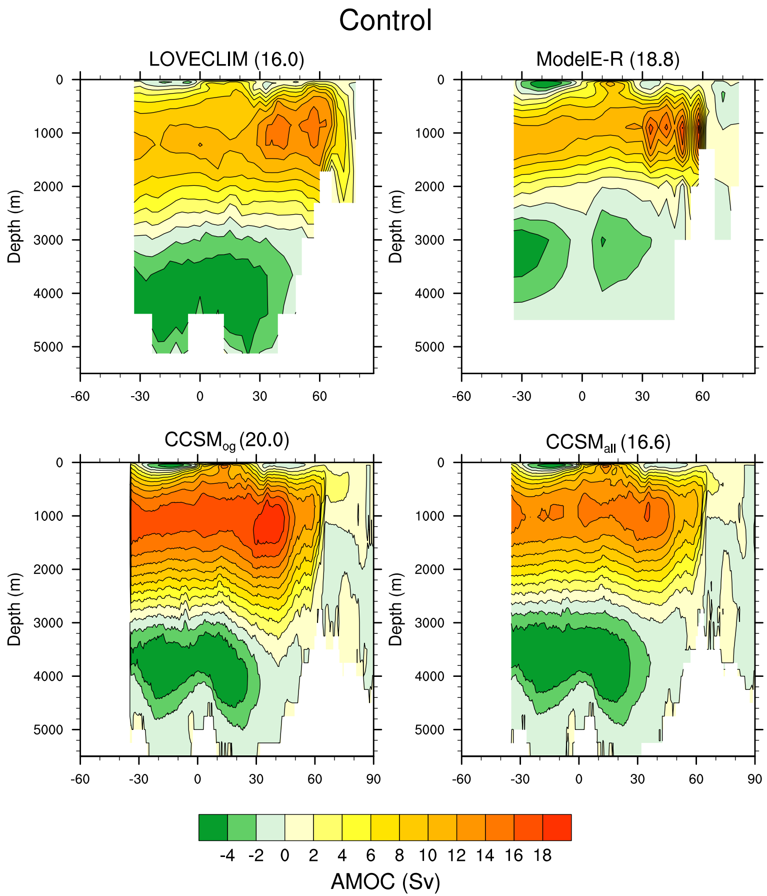

Fig. 1. The Atlantic meridional overturning streamfunctions of the control simulations (see Table 2), in Sv (1 Sv = 10^6 m^3 s^{-1}). Plotted values are 200-yr means except for CCSM$_{og}$, which is a 150-yr mean. Values in parentheses following the model names are long-term means for the maximum of the streamfunction below 500 m water depth.

CPD
8, 3949–3976, 2012

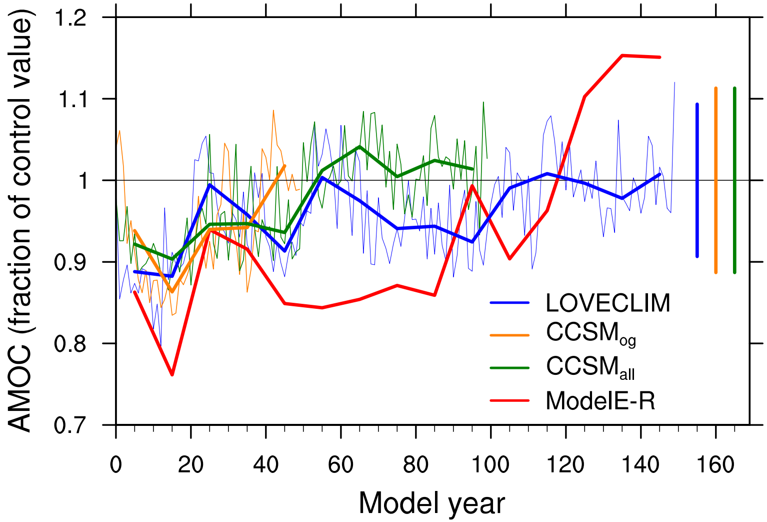

Fig. 2. Time series of AMOC intensity anomalies following the MWP, expressed as a fraction of the long-term control mean. The MWP of 2.5 Sv for one year was added at Model year 1. AMOC intensity is defined as the maximum value of the overturning streamfunction below 500 m water depth (excludes shallow wind-driven overturning). Heavy lines are decadal averages. Vertical lines on the right show the 2-σ range of interannual variability in the control simulations, and are not shown for ModelE-R since only 30-yr control averages are available.

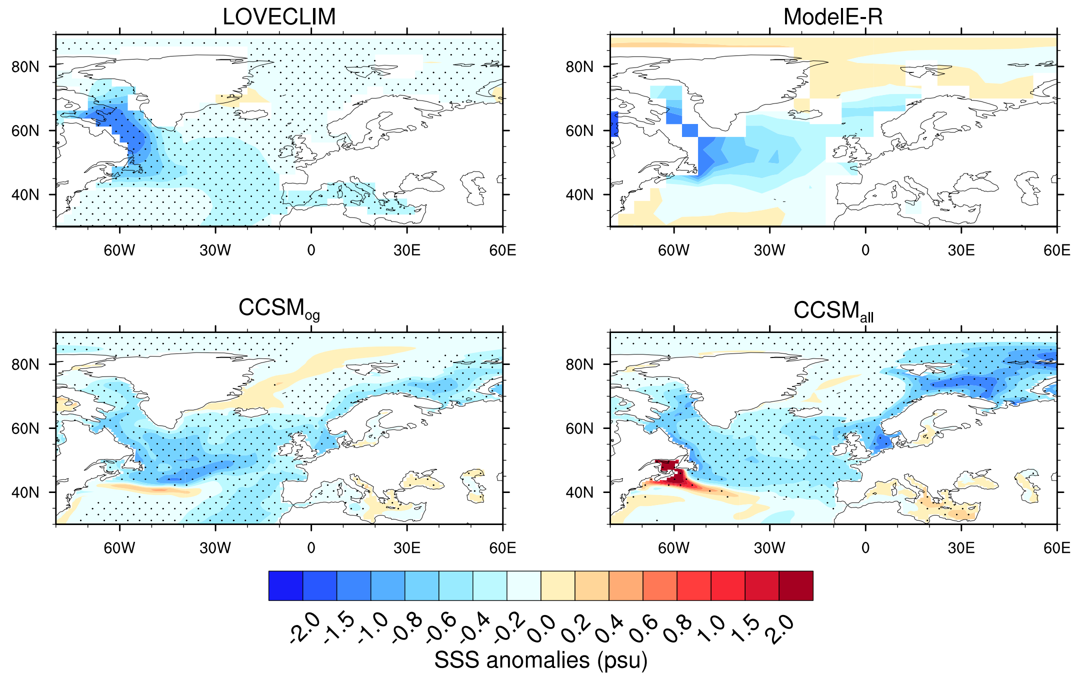

Fig. 3. Anomalies of annual-mean sea surface salinity in the first fifty years following the MWP relative to the control simulation, in practical salinity units. Stippling shows statistical significance at the 95 % level according to a Student's t-test. Statistical tests were not performed for ModelE-R since only decadal averages were available.

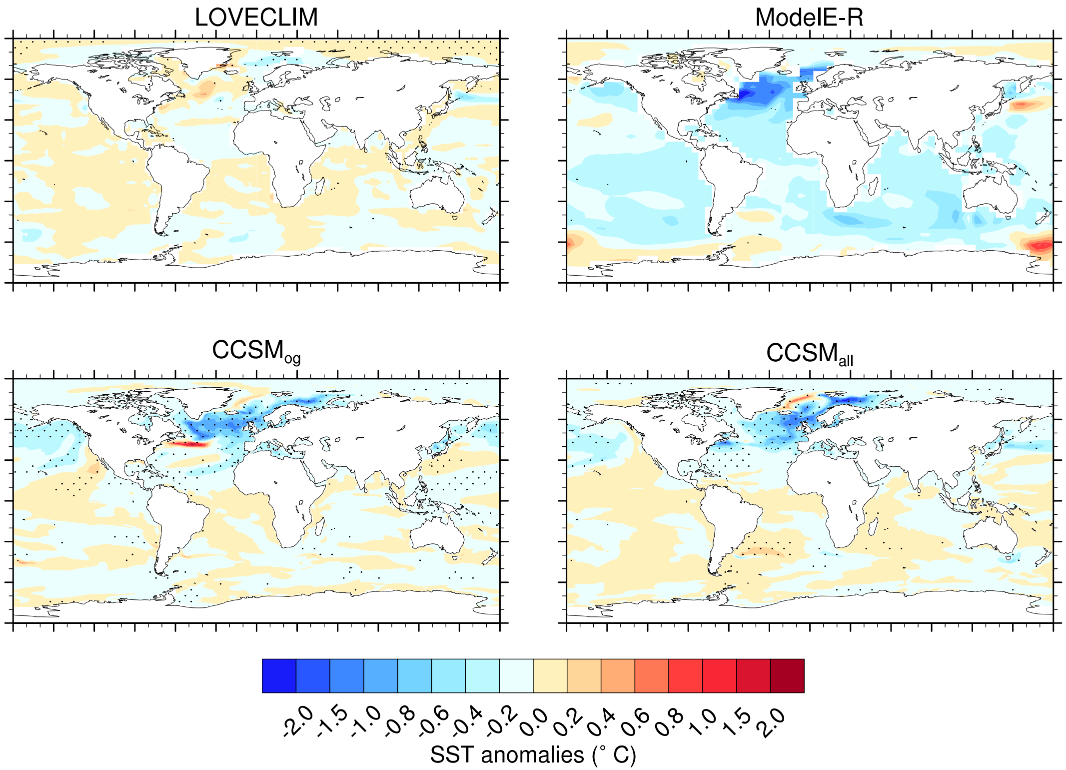

Fig. 4. Anomalies of annual-mean sea surface temperature in the first fifty years following the MWP relative to the control simulation, in degrees Celsius. Stippling shows statistical significance at the 95 % level according to a Student's t-test. Statistical tests were not performed for ModelE-R since only decadal averages were available.

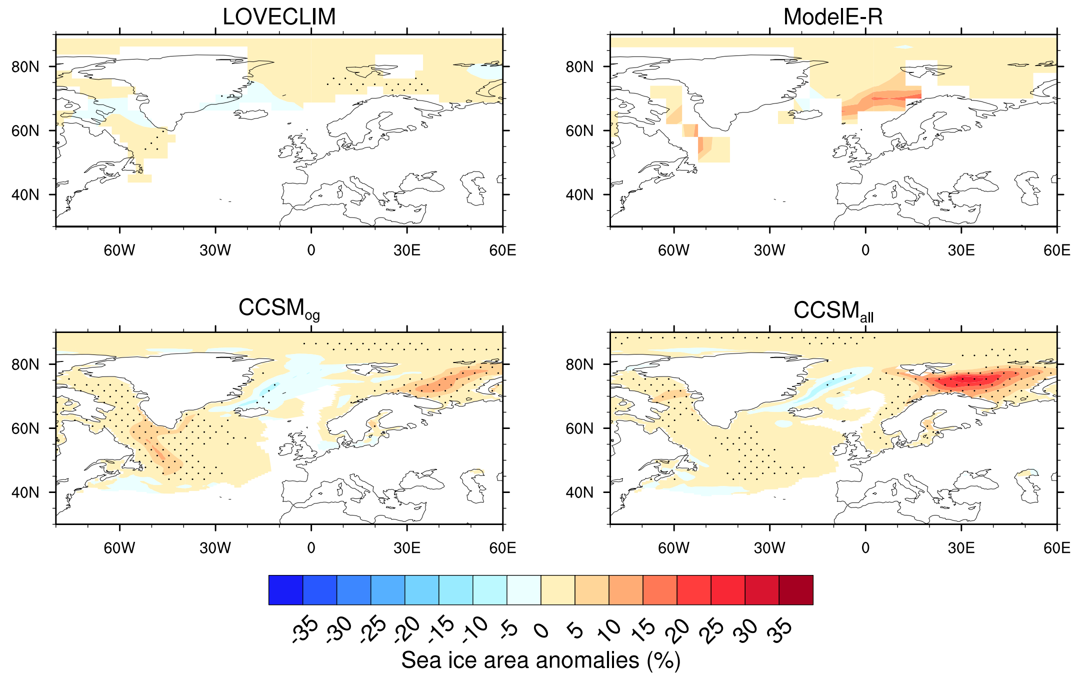

Fig. 5. Anomalies of annual-mean sea ice area in the first fifty years following the MWP relative to the control simulation, in percent. Stippling shows statistical significance at the 95 % level according to a Student's t-test. Statistical tests were not performed for ModelE-R since only decadal averages were available.

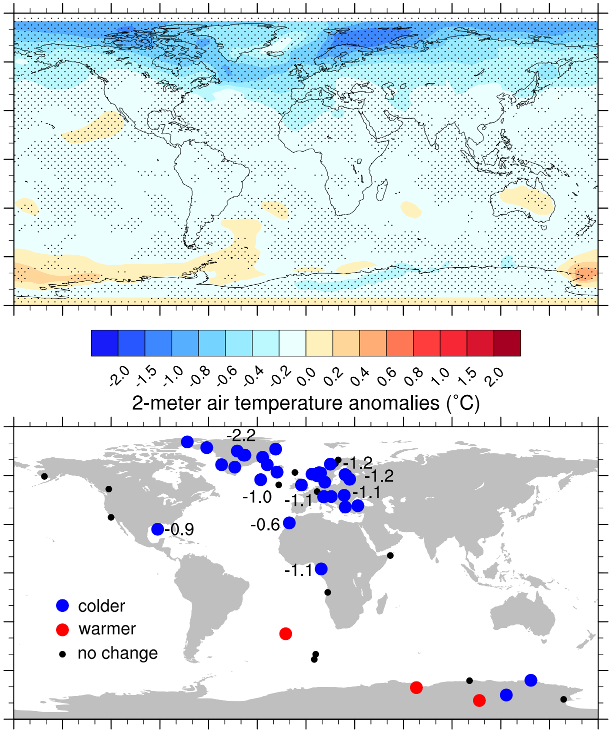

Fig. 6. Top panel: multi-model ensemble mean anomalies of annual-mean 2-meter air temperature in the first fifty years following the MWP relative to the control simulations, in degrees Celsius. Stippling shows grid cells where at least three of the simulations agree on the sign of the temperature anomaly. Bottom panel: qualitative and quantitative temperature anomalies, in degrees Celsius, inferred from proxy records for the 8.2 ka event, as summarized by Morrill et al. (2012).

CPD
8, 3949–3976, 2012

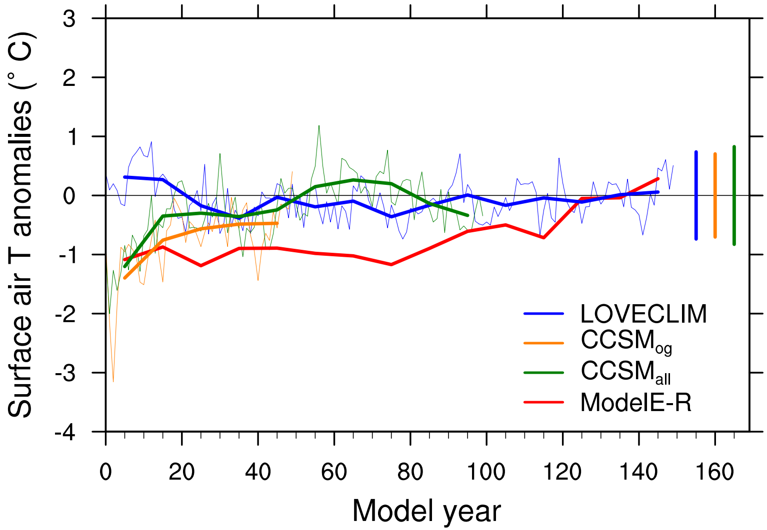

Fig. 7. Time series of annual-mean surface air temperature averaged over the region 50–70° N, 60° W–10° E in the North Atlantic, expressed as anomalies in degrees Celsius from the long-term control average. The MWP of 2.5 Sv for one year was added at Model year 1. Vertical lines on the right show the 2-σ range of interannual variability in the control simulations, and are not shown for ModelE-R since only 30-yr control averages are available.

CPD
8, 3949–3976, 2012

CPD
8, 3949–3976, 2012

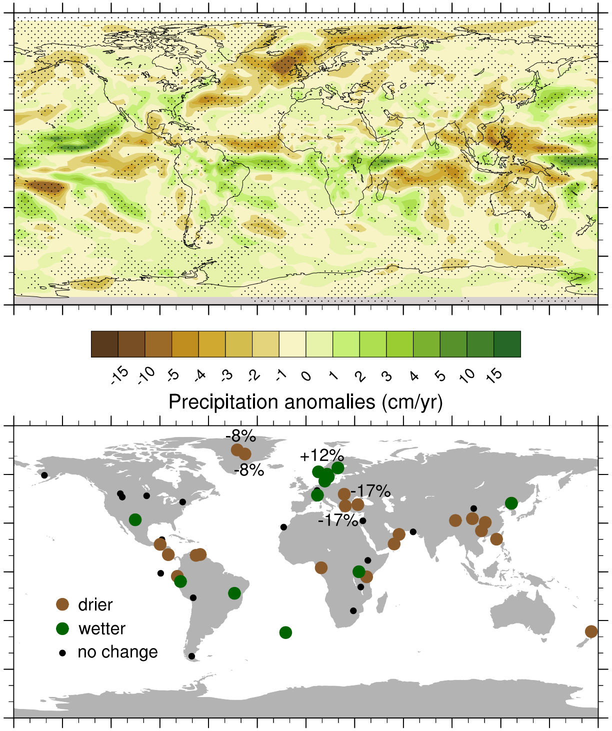

Fig. 8. Top panel: multi-model ensemble mean anomalies of annual-mean precipitation in the first fifty years following the MWP relative to the control simulations, in cm yr^{-1}. Stippling shows grid cells where at least three of the simulations agree on the sign of the temperature anomaly. Bottom panel: qualitative and quantitative precipitation anomalies, in % change from early Holocene background climate, inferred from proxy records for the 8.2 ka event, as summarized by Morrill et al. (2012).

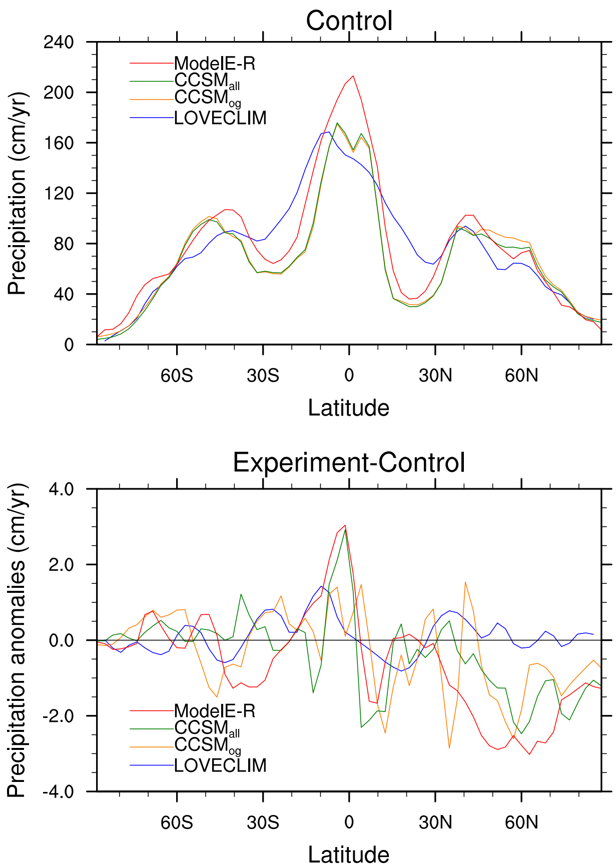

Fig. 9. Top panel: annual-mean precipitation zonally-averaged across the Atlantic (90° W–40° E) in the control simulation, in cm yr^{-1}. (Bottom) Anomalies of Atlantic annual-mean precipitation for the first fifty years following the MWP relative to the control simulation, in cm yr^{-1}.

CPD
8, 3949–3976, 2012